Plasmon excitation modes in nanowire arrays

M. S. Sander
Department of Chemistry, University of California, Berkeley, California 94720

R. Gronsky[a)]
Department of Materials Science and Engineering, University of California, Berkeley, California 94720

Y. M. Lin
Department of Electrical Engineering and Computer Science, Massachusetts Institute of Technology, Cambridge, Massachusetts 02139

M. S. Dresselhaus[b)]
Massachusetts Institute of Technology, Cambridge, Massachusetts 02139

(Received 9 June 2000; accepted for publication 10 November 2000)

Electron energy loss spectrometry and energy-filtered transmission electron microscopy reveal characteristic plasmon excitations in both isolated Bi nanowires and an array of Bi nanowires within an Al_2O_3 matrix. As the average nanowire diameter decreases from 90 to 35 nm, both the volume plasmon energy and peak width increase. In addition, a lower-energy excitation is present in a very localized region at the Bi–Al_2O_3 interface. These results are discussed in the context of quantum confinement and the influence of interfaces on the electronic properties of nanocomposite materials.
 [DOI: 10.1063/1.1337940]

INTRODUCTION

Nanowires have unique properties compared to bulk materials due to the restrictive two-dimensional confinement of their charge carriers. In clustered arrays of nanowires, there is sufficient wire cross section to carry high current, to enable handling without damage, and/or to provide redundancy for robust, failsafe applications. Consequently, arrays of nanowires in an insulating matrix hold promise for use in a variety of optical, electronic, and magnetic devices. The properties of such arrays are established by the familiar property-averaging laws for composites, but the large interfacial area associated with a nanowire array draws attention to its potential for influencing the properties of the composite in a significant way. Very little is known about the electronic properties of nanowire composites, and correlations with morphology are made difficult by the very high spatial resolution required to isolate single wires and their interfaces in stereological cross-sectional sampling.

Fortunately, the transmission electron microscope (TEM) easily meets the requirements for spatial resolution, and furthermore provides the capability for simultaneous imaging, diffraction, and spectroscopy from the same nanometer-scale volume element of the sample. Of special interest for studies of electronic properties is the electron energy loss spectroscopy (EELS) technique, which makes use of a magnetic-sector analyzer to disperse the electron beam across a broadband energy loss spectrum.[1] The low-loss regime of this spectrum (~0–40 eV) is dominated by valence electron excitations and can be related to the dielectric function of the material through a Kramers–Kronig analysis. In particular, EELS is useful for probing collective excitations of electrons (plasmons). Plasmon excitations are directly related to the band structure and electron density in the small volume of the sample probed by the focused electron beam.[2] Consequently, in dimensionally restricted materials, the position and width of the plasmon peak provide evidence of the influence of quantum confinement and surface effects on charge carriers. These effects have already been documented in studies of semiconducting and metal nanoparticles,[3–7] as manifested by a blueshift in the plasmon peak position and an increase in peak width as the particle diameter is decreased.

Plasmon excitations at interfaces have also been studied, because the electronic properties of interfaces directly affect the carrier mobility and scattering in a material. Studies of plasmons at planar interfaces and at nanoparticle interfaces have been used to assess interfacial chemistry and properties.[8–12] By coupling an EELS spectrometer with the powerful imaging capabilities of the TEM, it is also possible to select those electrons that have undergone a specific loss event during their transit through the sample and display the spatial variation of that loss event in an image. Such ''energy-filtered imaging'' of the plasmon excitations can be used to identify those regions of the sample that sustain a plasmon mode. Studies of plasmon delocalization have previously been used to assess interfacial composition and bonding in materials[13] and are particularly important for assessing properties in nanocomposite materials.

In this work we have studied plasmon excitations in bismuth nanowires arrayed within an alumina matrix. Because bismuth is a semimetal with a very small electron effective mass, the spatial extension of the electron wave functions is very large, affording bismuth some unique properties under conditions of reduced dimensionality. Quantum confinement effects become significant at relatively large sizes (~50 nm)

[a)]Electronic mail: rgronsky@socrates.berkeley.edu
[b)]Currently on leave.

compared to other semiconductors and metallic alloys. Due to its large band gap, the alumina matrix acts as an electrical and thermal insulator, making the bismuth–alumina system a model one for studying quantum confinement effects in nanowires. In addition, this system is promising for thermoelectric applications.[14]

Various properties of bismuth–alumina nanowire composite materials have been assessed previously, along with the composition and structure in the arrays. Below diameters of ~50 nm, magnetoresistance studies provide evidence of electron localization effects[15] and optical spectroscopy indicates a semimetal-to-semiconductor transition.[16] Magnetoresistance studies also indicate that wire-boundary (and not electron–electron) carrier scattering is the dominant carrier scattering mechanism in the arrays at low temperatures.[17] In addition, infrared reflectometry studies of the arrays indicate an absorption at $\sim 1000\ \mathrm{cm}^{-1}$, which is attributed to an intersubband transition in the bismuth nanowires that varies with wire diameter and incident polarization due to quantum confinement effects.[18] The array structure and composition were studied in the TEM, and it was determined that the wires are strongly textured along the wire axis, with high-aspect ratio grains. Compositional analysis in the TEM revealed that the bismuth–alumina interface is chemically abrupt, with an interphase region of less than 1 nm.[19]

The goal of this work is to understand the relative contributions to the electronic properties of a nanowire array from both the individual nanowires and their wire–matrix interfaces. We report on the behavior and localization of the plasmons in bismuth nanowires arrayed within an alumina matrix. We discuss the results in the context of the structure, composition, and properties of these nanocomposite materials.

EXPERIMENTAL METHODS

Nanowire arrays were prepared by pressure injection of molten Bi into porous anodic alumina templates. Through control of the anodization conditions, templates with varying pore diameters were produced. The pressure injection and template fabrication processes are described in detail elsewhere.[20]

Two types of specimens were prepared for TEM studies. Individual wires were isolated by selectively etching the template in a solution of 45 g/l CrO_3 in 3.5% H_3PO_4. Etching was terminated by dilution and the wires remained suspended in ethanol. TEM specimens were prepared by dispersing this solution directly onto holey carbon films suspended over copper grids. Specimens of dispersed individual wires were transferred to the microscope immediately after preparation in order to minimize surface oxidation. A surface oxide layer less than 1 nm thick was observed on the individual wires by high resolution TEM. In order to investigate the Bi–Al_2O_3 interface, cross-sectional specimens were prepared by mechanically dimpling and ion milling the nanowire arrays.

The EELS studies were performed in a Philips CM200 TEM at 200 kV with a probe size of approximately 1.2 nm. The data were collected at 0.1 eV/channel with a GATAN 666 PEELS spectrometer and corrected for dark current and noise. Energy-filtered images were obtained with an energy slit of 5 eV centered on the selected energy loss peak.

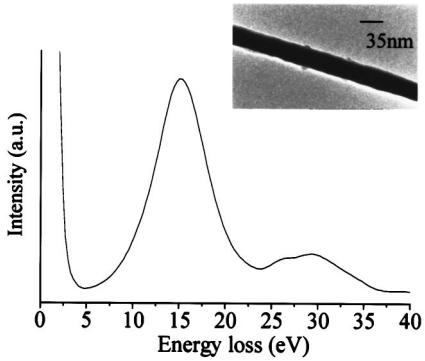

FIG. 1. Electron energy loss spectrum from the center of a bismuth nanowire, with an inset TEM image of a wire.

RESULTS AND DISCUSSION

In order to determine the effect of the wire diameter on plasmon excitations in nanowire arrays, we collected electron energy loss spectra from individual bismuth nanowires with different diameters. A TEM image of one such nanowire and its corresponding EELS spectrum are shown in Fig. 1. The largest feature in the loss spectrum is ascribed to the volume plasmon, which has a value of ~14 eV for bulk bismuth.[21] Two higher-energy loss events are those discernible at ~26 and ~29 eV, and these are identified as the $O_{4,5}$ ionization edges. There is no significant contribution to the spectrum from the 10 eV surface plasmon of bulk bismuth. However, in order to isolate the volume plasmon signal in the individual nanowires with minimal surface effects, the 1.2 nm incident electron probe was focused on the wire center during data acquisition.

Electron energy loss spectra were collected from wires with three different diameters, nominally 90, 60, and 35 nm,

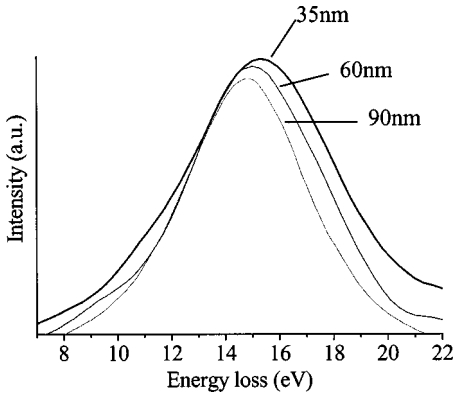

FIG. 2. Series of electron energy loss spectra taken from the center of bismuth nanowires with nominal diameters of 35, 60, and 90 nm. The volume plasmon peaks are scaled to approximately the same maximum intensity in order to highlight the shift in peak position as a function of wire diameter.

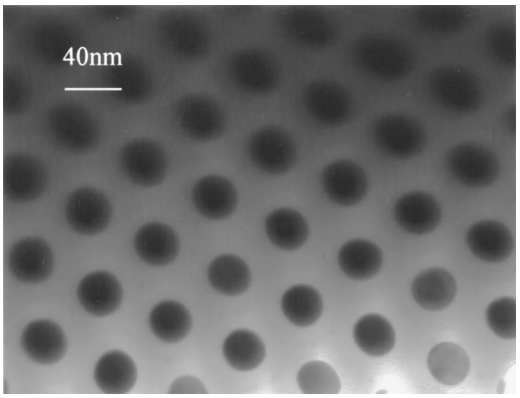

FIG. 3. Cross-sectional TEM image of a bismuth nanowire array in an alumina matrix. The average wire diameter is ~35 nm.

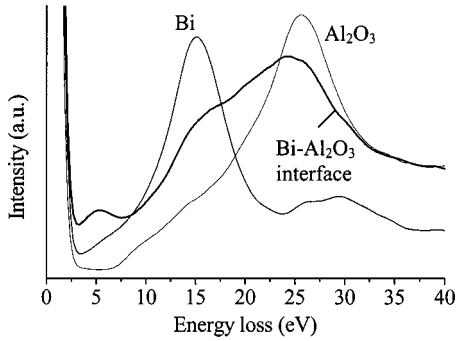

FIG. 4. Electron energy loss spectra from the nanowire array, recorded with a 1.2 nm probe size positioned in the Bi, Al_2O_3, and at the Bi/Al_2O_3 interface.

as verified in TEM images. Representative spectra from all three wire sizes are shown in Fig. 2.

It is apparent that there is a slight increase in the plasmon peak maximum energy with decreasing wire diameter. There are several potential factors that may contribute to the shift in peak energy. As the wire diameter is decreased, the charge carriers are increasingly confined. In both metal[3,4] and semiconductor[5–7] nanostructures, a blueshift in the plasmon energy with decreasing diameter has been attributed to carrier confinement. In these systems, the energy shifts occur at much smaller diameters than in the bismuth nanowires studied here: less than 10 nm as compared to greater than 35 nm in the bismuth wires. Because of bismuth's very small effective mass, it is possible that quantum confinement affects the plasmon energy at these relatively large diameters. However, there are also other potential sources of the energy shift. From TEM imaging experiments on the pressure injected wires, localized strain fields within the wires were identified.[19] Because of the very narrow diameters, the amount of strain is difficult to quantify. If there is increased strain in the smaller diameter wires, this may contribute to the shift in plasmon energy. Finally, surface contributions cannot be ruled out. The spectra were taken using a ~1 nm probe focused at the wire center in order to minimize surface effects, but surface processes do contribute to an increase in the peak width, as described below. It is clear that a more thorough study of the dependence of the plasmon energy on wire diameter is required in order to assess the influence of each of these possible effects.

In addition to an increase in the volume plasmon energy, there is also a slight broadening of the volume plasmon peak with decreasing wire diameter. This behavior is attributed to an increase in surface excitations and scattering. The decay of the volume plasmon to surface processes becomes more pronounced when the surface-to-volume ratio increases. Therefore this trend is more significant in nanoparticles with much smaller sizes[4–6] than in the wires studied here.

In order to assess interfacial contributions to electron excitations within the composite, the electron probe was used to sample areas from an array of 35 nm wires in cross section, as shown in Fig. 3. Electron energy loss spectra were collected from 1 nm regions in the Bi, the alumina, and at the Bi–Al_2O_3 interface, as shown in Fig. 4. The spectrum taken at the interface includes contributions from the bismuth and alumina bulk plasmons, as well as a ~5.5 eV peak, at much lower energy than the ~10 eV expected for bismuth surface plasmons. A shift to lower energy is expected at the interface with an oxide, as observed at planar interfaces[8,9] as well as nanostructure–oxide interfaces.[10–12] The condition for resonance at planar interfaces between two materials **A** and **B** is $\varepsilon_{1A}(\omega)+\varepsilon_{1B}(\omega)=0$.[1] While the dielectric functions for the bismuth nanowires and templates have not been determined, 5.5 eV is a reasonable energy to expect for an interface plasmon based on the bismuth[21] and alumina[22] bulk values.

To determine the spatial variation of the excitations, energy-filtered imaging was employed. The zero-loss image, along with the contributions from the bismuth plasmon at 15.5 eV and alumina plasmon at 26 eV are shown by the bright areas in Figs. 5(a), 5(c), and 5(d). An image created from the lower energy 5.5 eV peak [Fig. 5(b)] indicates that this excitation is very sharply localized at the wire–matrix interface. In previous work, we have shown using core-loss EELS in the TEM that the wire/matrix interface in the arrays is abrupt, with evidence of Bi–O bonding in less than a 1 nm wide region at the interface.[19] In future work, it may be possible to correlate compositional information with interfa-

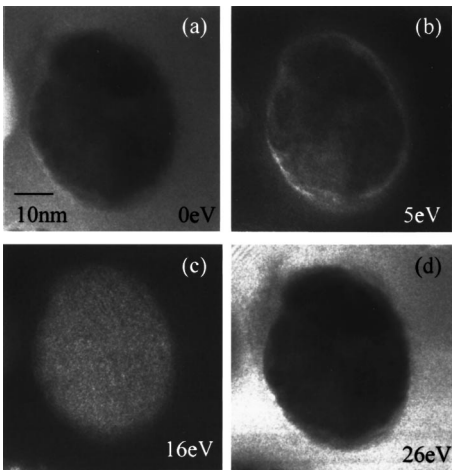

FIG. 5. Series of energy filtered images from a bismuth nanowire array formed with a 5 eV energy slit centered at (a) 0 eV, (b) 5 eV, (c) 16 eV (after removing the contribution from the alumina loss peak), and (d) 26 eV.

cial plasmon spatial variation results in order to understand better how these factors are related to interface bonding and array behavior.

CONCLUSIONS

We have investigated the electron energy loss excitations in bismuth nanowires and at the $Bi-Al_2O_3$ interface in bismuth nanowire arrays. As the wire diameter decreases, there is an increase in the volume plasmon energy. This increase in volume plasmon energy occurs at much larger diameters ($\sim$35 nm) for bismuth wires than in other previously studied metal and semiconductor nanoparticles. Several potential origins of this shift are discussed, including quantum confinement effects, localized strain within the wires, and interface effects. There is also a slight broadening in the peak width for narrower wires, which is attributed to more rapid decay of the volume plasmon with the increased surface-to-volume ratio. In EELS spectra from the $Bi-Al_2O_3$ interface there is a low energy loss peak at $\sim$5.5 eV, consistent with an interface plasmon excitation. This excitation is strongly localized within a narrow region ($<$3 nm) at the interface, as evidenced by energy-filtered imaging. These results demonstrate the usefulness of EELS and energy-filtered imaging to assess the electronic properties of nanostructures and nanocomposite materials at high spatial resolution ($\sim$1 nm). This type of study will allow for a more thorough understanding of the relationship between local electronic excitations and nanocomposite material properties.

ACKNOWLEDGMENTS

This work was funded by the Office of Naval Research through a Multi-University Research Initiative under Contract No. N00014-97-1-0516. Electron microscopy was performed at the National Center for Electron Microscopy (NCEM), Lawrence Berkeley National Laboratory. Technical assistance from C. Nelson (NCEM) and helpful discussions with M. R. Black (MIT) are also gratefully acknowledged.

[1] R. F. Egerton, *Electron Energy-Loss Spectroscopy in the Electron Microscope*, 2nd edition (Plenum, New York, 1996).
[2] H. Raether, *Excitation of Plasmons and Interband Transitions by Electrons* (Springer, Berlin, 1980).
[3] A. vom Felde, J. Fink, and W. Ekardt, Phys. Rev. Lett. **61**, 2249 (1988).
[4] W. Ekardt, Phys. Rev. B **31**, 6360 (1985).
[5] M. Mitome, Y. Yamazaki, H. Takagi, and T. Nakagiri, J. Appl. Phys. **72**, 812 (1992).
[6] B. W. Reed, J. M. Chen, N. C. MacDonald, J. Silcox, and G. F. Bertsch, Phys. Rev. B **60**, 5641 (1999).
[7] P. N. H. Nakashima, T. Tsuzuki, and A. W. S. Johnson, J. Appl. Phys. **85**, 1556 (1999).
[8] H. Fukuda, M. Yasuda, and T. Iwabuchi, Appl. Phys. Lett. **61**, 693 (1992).
[9] M. A. Turowski, T. F. Kelly, and P. E. Batson, J. Appl. Phys. **76**, 3776 (1994).
[10] S. Munnix and M. Schmeits, Phys. Rev. B **32**, 4192 (1985).
[11] T. Stockli, P. Stadelmann, and A. Chatelain, Microsc. Microanal. Microstruct. **8**, 145 (1997).
[12] D. Ugarte, C. Colliex, and P. Trebbia, Phys. Rev. B **45**, 4332 (1992).
[13] Z. L. Wang and A. J. Shapiro, Ultramicroscopy **60**, 115 (1995).
[14] Y.-M. Lin, X. Sun, and M. S. Dresselhaus, Phys. Rev. B **62**, 4610 (2000).
[15] Z. Zhang, X. Sun, M. S. Dresselhaus, J. Y. Ying, and J. P. Heremans, Appl. Phys. Lett. **73**, 1589 (1998).
[16] Z. Zhang, J. Y. Ying, and M. S. Dresselhaus, J. Mater. Res. **13**, 1745 (1998).
[17] Z. Zhang, X. Sun, M. S. Dresselhaus, J. Y. Ying, and J. Heremans, Phys. Rev. B **61**, 4850 (2000).
[18] M. R. Black, M. Padi, S. B. Cronin, Y.-M. Lin, O. Rabin, T. McClure, G. Dresselhaus, P. L. Hagelstein, and M. S. Dresselhaus, Appl. Phys. Lett. **77**, 4142 (2000).
[19] M. S. Sander, Y. M. Lin, M. S. Dresselhaus, and R. Gronsky, *Material Research Society Symposium Proceedings: Nanophase and Nanocomposite Materials III*, Boston, MA, 2000 (Mater. Res. Soc., Pittsburgh, PA, 2000), pp. 681, 213.
[20] Z. B. Zhang, D. Gekhtman, M. S. Dresselhaus, and J. Y. Ying, Chem. Mater. **11**, 1659 (1999).
[21] C. Wehenkel and B. Gauthe, Solid State Commun. **15**, 555 (1974).
[22] E. D. Palik, *Handbook of Optical Constants of Solids III* (Academic, San Diego, CA, 1998).